CHAPTER 14

Heat and Mass Transfer in Food Processing

Mohammed Farid
University of Auckland, Auckland, New Zealand

1. BASIC CONCEPTS OF HEAT AND MASS TRANSFER

Understanding heat transfer in food processing is important for the development of energy efficient thermal processes and insures the production of safe and high-quality food. The food industry is known for its high consumption of energy in processes such as sterilization, evaporation, and drying. Generally, heat transfer is governed by the three well-known modes of transport—conduction, convection, and radiation. However, radiation is important only in high temperature applications such as baking and grilling.

Heat transfer in food processing is complicated by the occurrence of simultaneous heat and mass transfer in drying and frying, free convection heat transfer in thermal sterilization of cans, and phase change in freezing and thawing. Sterilization, drying, and thawing processes will be discussed in some detail in this chapter. First, the fundamentals of heat and mass transfer are briefly introduced. For more detailed analysis, the readers can consult the literature on heat transfer (Holman, 1992; Mills, 1992) and mass transfer (Treybal, 1980).

In many applications, heat transfer is accompanied by mass transfer of moisture or nutrients. Air drying, freeze drying, spray drying, and steam drying are accompanied by moisture transfer, which also undergoes phase change (evaporation). Heat transfer, together with moisture and vapor transfer, controls these processes. Other phase change operations, such as evaporation and condensation, are common in the food industry, mainly to concentrate liquid foods such as milk and juices.

Concentration of liquid foods may also be done using a freeze concentration process in which some of the water is frozen leaving a concentrated solution. Mass transfer of moisture and nutrients may occur independently of heat transfer in osmotic

Handbook of Farm, Dairy and Food Machinery Engineering
DOI: http://dx.doi.org/10.1016/B978-0-12-385881-8.00014-8
© 2013 Elsevier Inc.
All rights reserved.

dehydration, membrane separation, absorption, adsorption, and many other processes, and will not be discussed in this chapter.

During heating, food products undergo various chemical and biological changes at rates that are a function of temperature. In contrast to usual chemical reactions, the chemical and biological reactions associated with food processing do not generate large amounts of heat and hence these changes can be decoupled from the differential equations describing heat transfer, and hence the analysis is significantly simplified.

Food is dried with hot air or superheated steam, fried in hot oil, and usually sterilized in cans or pouches with steam. Heat is transferred from the heating fluid to the surface of the material by free or forced convection. With solid food, heat is transferred by conduction whereas vapor is transported by diffusion or other mechanisms through the pores of the food. For liquid food in containers, natural convection rather than conduction dominates heat transfer. Thawing of products such as meat is usually done in a hot air environment or by using hot water. However, microwave and radio frequency may also be used to assist in thawing of meat, as discussed later in this chapter. Microwaves and radio frequency waves have the ability to penetrate deep inside the food, producing heat within the material. Vacuum microwave drying is sometimes applied to heat sensitive food so that evaporation occurs at temperatures well below 100°C, thus minimizing serious damage caused by high temperature applications (Mousa and Farid, 2002).

In freezing and thawing, heat transfer occurs with minimum mass transfer but with a moving interface separating the frozen and thawed regions, which causes nonlinearity in the mathematical analysis of the associated heat transfer.

In cooking, food is usually boiled in water. Heat is transferred from water to the surface of the food with a high boiling heat transfer coefficient and hence it is safe to assume that most of the heat transfer resistance lies within the food itself. This is the same in frying, where water is boiled within the food being deep fried. If a meat patty is grilled in a direct fire, then heat is transferred to its surface mainly by radiation, but when it is grilled between two hot plates, as is usually done in the fast food industry, heat will be mainly transferred by conduction. Ohmic cooking and heating is an efficient means of heating liquid and solid products. For example, a meat patty is conductive to electricity and so if a voltage is applied across two of its surfaces, an electrical current will pass through it generating heat internally, which will assist cooking (Ozkan *et al.*, 2004).

In the following section, the three modes of heat transfer are briefly presented, with a short introduction to mass transfer. For detailed analysis, the reader should consult the literature on heat and mass transfer (Holman, 1992; Mills, 1992; Treybal, 1980).

1.1 Conduction Heat Transfer

Steady-state heat transfer in solids is governed by Fourier's Law, which states that the heat flow (q) is directly proportional to the temperature gradient in the solid:

$$q = -kA\frac{dT}{d\gamma} \qquad [14.1]$$

where T is the temperature, A is the area perpendicular to heat flow, y is the position in the direction of heat flow, and k is the thermal conductivity of the material, which has values ranging from <0.1 W m^{-1} K^{-1} for dried food product to 0.5 W m^{-1} K^{-1} for most foods. For comprehensive information on the values of thermal conductivity of food products, see Shafiur (1995).

Steady-state heat conduction has limited application in food processing, as all these processes are transient in nature. However, Eq. 14.1 is useful for specific calculations, for example, those related to the estimation of heat gain in cold storage.

The 1-D unsteady-state heat transfer in a solid may be expressed as

$$\frac{\partial T}{\partial t} = \left(\frac{\alpha_{th}}{\gamma^n}\right)\left(\frac{\partial}{\partial \gamma}\left[\gamma^n \frac{\partial T}{\partial \gamma}\right]\right) \qquad [14.2]$$

In Eq. 14.2, α_{th} is the thermal diffusivity of the material and is equal to k/ρCp, where ρ is the density, and Cp is the specific heat capacity of the material. For rectangular coordinates, $n = 0$, for cylindrical coordinates, $n = 1$ and $\gamma =$ r, and for spherical coordinates, $n = 2$ and $\gamma =$ r. The equation can be expanded to cover multi-dimensions, as discussed in most heat transfer textbooks.

Analytical solutions to the above equation are available for very limited boundary conditions and geometry. Simplified methods such as those based on Heissler's Charts (Holman, 1992) use the available 1-D solution to generate a solution for multi-dimensional problems. However, with the availability of high speed computers and efficient numerical methods (finite difference, finite element, and finite volume), the unsteady-state heat conduction could be solved for almost any geometry and any boundary conditions. These numerical solutions will provide information on the transient temperature distribution within the food, which is important for the determination of food sterility and quality. This is specifically important when the Biot number (hL/k) is >0.1, where h is the heat transfer coefficient, and L is a characteristic dimension (slab half thickness or radius of long cylinder and sphere). When the Biot number is <0.1, it is possible to ignore the temperature distribution and assume that the solid is at uniform temperature. Under such conditions, the lumped heat capacity analysis may be applied to simplify the above equation:

$$mCp\frac{dT}{dt} = hA(T_\infty - T) \qquad [14.3]$$

where m and A are the mass and surface area of the body and T_∞ is the heating or cooling fluid temperature. Eq. 14.3 on integration gives

$$\frac{T - T_\infty}{T_i - T_\infty} = \exp\left(-\frac{hA}{mCp}t\right) \quad [14.4]$$

where T_i is the initial temperature and t is the time. Eq. 14.4 provides a quick estimate of the time required for food heating or cooling when there is no phase change and no significant temperature distribution within the solid food.

1.2 Forced Convection Heat Transfer

Convection heat transfer from or to the surface of a material at T_s may be calculated using Newton's Law of cooling:

$$q = hA(T_s - T_\infty) \quad [14.5]$$

Forced convection heat transfer is associated with fluid flow such as in blast freezing and air drying, where cold or hot air is supplied by means of a blower to extract heat from the food product in freezing or provide heat to the food product in drying. The forced convection heat transfer coefficient is calculated from empirical correlation of the form:

$$Nu = c\mathrm{Re}^n\ \mathrm{Pr}^m \quad [14.6]$$

In the above equation, the Nusselt number (Nu) is hL/k, the Reynolds number (Re) is ρuL/μ, and the Prandtl number (Pr) is Cpμ/k. The constants in the above correlation are given in the literature (Holman, 1992; Mills, 1992) for a large number of geometry and flow conditions.

1.3 Free Convection Heat Transfer

Free convection current is usually established solely as a result of heat transfer and not via the use of externally forced flow. The motion is induced by the density difference in the gas or liquid caused by temperature difference. There are large numbers of food heating and cooling applications in which free convection is the dominant mode of heat transfer. Free convection heat transfer controls the process of sterilization of food in cans and meat freezing in still air or brine. Newton's Law of cooling (Eq. 14.5) describes heat transfer from the fluid to the surface of the food, but the coefficient is calculated based on the following correlation (or many other more complicated forms of the equation):

$$Nu = cRa^n\ \mathrm{Pr}^m \quad [14.7]$$

where Rayleigh number (Ra) is $(T_s - T_\infty)\ \beta g\rho L^3/\alpha\mu$, in which β is the volumetric thermal expansion coefficient of the fluid.

Boiling and condensation heat transfer can occur in free and forced convection environments. Empirical correlations are available in the literature for the calculation of the relevant coefficients.

1.4 Radiation Heat Transfer

Thermal radiation is a different mode of heat transfer, requiring no atmosphere for its transfer. Oven baking and cooking of food is controlled by radiant heat generated from the heating element, a flame, or the walls of an oven. Food will receive heat also by natural or forced convection but radiation will be the dominant mode of heat transfer. A black surface is defined as the surface which absorbs all incident radiation ($\varepsilon = 1.0$). Very polished surfaces reflect most of the incident radiation and usually have *emittance* (ε) < 0.1. Real surfaces, including those of food products, have *emittances* lying between these two extreme values. The fraction of incident radiation absorbed by the surface is called *absorptance*. The surface of most food may be assumed a *gray surface*, which is defined as the surface having constant *absorptance* irrespective of the nature of radiation (Mills, 1992). For such gray surfaces, the following equation may be used to calculate heat exchange from surface 1 to 2:

$$q_{12} = \sigma A_1 F_{12}(T_1^4 - T_2^4) \qquad [14.7a]$$

where σ is Stefan-Boltzmann constant (5.67×10^{-8} W m^{-2} K^{-4}) and F_{12} is a *shape factor*, which depends on emittance and geometry (Mills, 1992). Determining the shape factor is difficult, as described in the literature (Holman, 1992; Mills, 1992). For the special case of A_1 being small relative to A_2 or surface 2 is almost black, Eq. 14.7a will simplify to

$$q_{12} = \sigma \varepsilon_1 A_1(T_1^4 - T_2^4) \qquad [14.7b]$$

where ε_1 is the emittance of surface 1.

1.5 Mass Diffusion

Under steady-state conditions, the diffusion of moisture and nutrients in food may be described by Fick's First Law:

$$m_a = -DA\frac{dC_a}{dy} \qquad [14.8]$$

where m_a is the mass flow in kgs^{-1}, D is the diffusion coefficient in m^{2}s^{-1}, and C_a is the concentration of the diffusing materials in kg m^{-3}. The flux is sometimes expressed in moles instead of mass.

Eq. 14.8 is identical to Eq. 14.1, which describes steady-state heat conduction and it may be used to describe steady-state diffusion of gaseous or liquids. By analogy with heat transfer, Eq. 14.2 may be used to describe the unsteady-state mass diffusion (Fick's Second Law) by replacing the temperature with concentration and the thermal diffusivity α_{th} by mass diffusivity $\alpha_{m.}$. In mass diffusion of species in fluids, the diffusion coefficient D is the molecular diffusion coefficient, whereas in porous foods its magnitude can be different from molecular diffusion coefficients by an order of magnitude. This effective diffusion coefficient, which is a function of moisture content and the structure of the porous food, in processes such as drying, is well discussed in the literature.

1.6 Mass Transfer by Convection

Nutrient or moisture diffuses inside the pores of the food at a rate of m_a, according to Fick's Law and then is transported from or to the surface by convective mass transport, similar to heat transport by free convection:

$$m_a = h_m A(C_s - C_\infty) \qquad [14.9]$$

where h_m is the mass transfer coefficient and C_s and C_∞ are the species concentrations at the surface of the food and in the bulk of the fluid.

The mass transfer coefficient h_m is calculated from empirical correlations available in the literature (Treybal, 1980). These correlations are based on the analogy between heat and mass transfer, which transforms Eq. 14.6, written for heat transfer, into the following form, written for mass transfer:

$$Sh = cRe^n Sc^m$$

where the Sherwood number (Sh) is h_mL/D and the Schmidt number (Sc) is μ/ρL.

The remainder of this chapter will present three case studies of food processing in which heat transfer plays a major role, but in ways different from those normally experienced.

2. CASE STUDY 1: THERMAL STERILIZATION USING COMPUTATIONAL FLUID DYNAMICS

Two different methods of thermal sterilization are known, the aseptic processing in which the food product is sterilized prior to packaging, and canning in which the product is packed and then sterilized. For liquid food heated in a can, free convection of fluid occurs because of the density differences of the fluid caused by the temperature gradient within the can. For solid food with conduction heating, the location of the slowest heating zone (SHZ) can be determined theoretically and experimentally, as it lies always at the geometric center of the can. However, for liquid food, the

determination of the SHZ is difficult because of the complex nature of natural convection heating, which requires numerical solutions of partial differential equations, describing fluid motion and heat transfer. Measuring the temperature distribution using thermocouples at different positions will disturb the flow patterns and affect the correct prediction of the true location of the SHZ.

The partial differential equations governing natural convection motion of the liquid food in a cylindrical space are the Navier-Stokes equations in cylindrical coordinates (Ghani *et al.*, 1999a and b) as shown below:

$$\textit{Continuity equation} \quad \frac{1}{r}\frac{\partial}{\partial r}(r\rho_f v_r) + \frac{\partial}{\partial r}(\rho_f v_z) = 0 \qquad [14.10]$$

$$\textit{Energy conservation} \quad \frac{\partial T}{\partial t} + v_r\frac{\partial T}{\partial r} + v_z\frac{\partial T}{\partial z} = \frac{k_f}{\rho_f Cp_f}\left[\frac{1}{r}\frac{\partial}{\partial r}\left(r\frac{\partial T}{\partial r}\right) + \frac{\partial^2 T}{\partial z^2}\right] \qquad [14.11]$$

Momentum equation in the vertical direction

$$\rho_f\left(\frac{\partial v_z}{\partial t} + v_r\frac{\partial v_z}{\partial r} + v_z\frac{\partial v_z}{\partial z}\right) = -\frac{\partial p}{\partial z} + \mu\left[\frac{1}{r}\frac{\partial}{\partial r}\left(r\frac{\partial r_z}{\partial r}\right) + \frac{\partial^2 v_z}{\partial z^2}\right] + \rho_f g \qquad [14.12]$$

Momentum equation in the radial direction

$$\rho_f\left(\frac{\partial v_r}{\partial t} + v_r\frac{\partial v_r}{\partial r} + v_z\frac{\partial v_r}{\partial z}\right) = -\frac{\partial p}{\partial z} + \mu\left[\frac{\partial}{\partial r}\left(\frac{1}{r}\frac{\partial}{\partial r}(rv_r)\right) + \frac{\partial^2 v_r}{\partial z^2}\right] \qquad [14.13]$$

where T is the temperature, P is the pressure, t is the heating time, g is the gravitational acceleration, μ is the apparent viscosity, ρ_f is the density of the fluid, Cpf is the specific heat of the fluid food, k_f is the thermal conductivity of the fluid food, and v_r and v_z are the velocity components in the radial and axial direction, respectively.

Based on the Boussinesq approximation, the density of the fluid p_f can be written as

$$\rho_f = \rho_o[1 - \beta(T - T_o)] \qquad [14.14]$$

where β is the thermal expansion coefficient of the liquid and T_o and ρ_o are the temperature and density at the initial condition. The density is assumed constant in the governing equations except in the buoyancy term (Boussinesq approximation), where Eq. [14.13] is used to describe its variation with temperature.

The above equations are written for the vertical can. For horizontal cans and pouches, the formulation becomes three-dimensional. These formulations are not presented here but discussed in detail in Ghani *et al.* (2001, 2002).

2.1 Simulations of Thermal Sterilization in a Vertical can

Sterilization of liquid food contained in a metal can, in an upright position and heated at 121°C by steam from all sides, was theoretically modeled and the published results (Ghani *et al.*, 1999a,b) are presented in this chapter. Sodium carboxy-methyl cellulose (CMC) was used as the model liquid. The objective of the simulation was to study the effect of natural convection current on the movement of the SHZ during sterilization. The computations were performed for a can with a radius of 40.5 mm and a height of 111 mm. A non-uniform grid system was used in the simulation with 3,519 cells: 69 in the axial direction and 51 in the radial direction, graded in both directions with a finer grid near the wall. The natural convection heating of CMC was simulated for 2,574s. Because of the axisymmetry of the cylindrical can used in the simulation, heat transfer was simplified into a 2-D problem.

Figure 14.1 shows the temperature profile, velocity vector, and flow pattern of the CMC in a can heated by steam condensing along its outside surface. Figure 14.1(a) shows the influence of natural convection current on the movement of the SHZ in the can (i.e. the location of the lowest temperature at a given time). Figure 14.1(a) shows that the location of the SHZ is not at the geometric center of the can as in the case of conduction heating. As heating progresses, the SHZ is pushed more toward the bottom of the can. The SHZ keeps moving during heating and eventually stays in a region that is about 10−12% of the can height from the bottom. Figure 14.1(b) and (c) shows the recirculating secondary flow created by the buoyancy force, which occurs as a result of temperature variation (from the wall to the core).

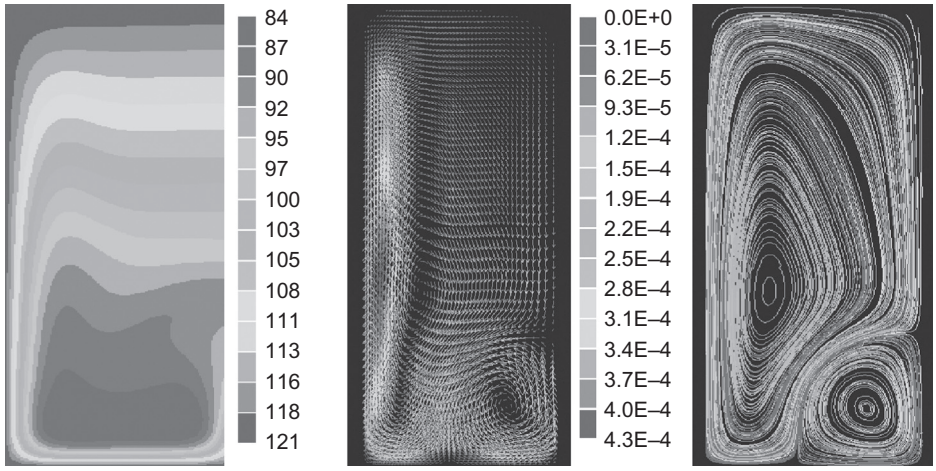

Figure 14.1 ***Temperature profile, velocity vector, and flow pattern of CMC in a vertical can heated by condensing steam after 1,157s. The right-hand side of each figure is centerline (Ghani et al., 1999b).***

2.2 Simulation of Bacteria Deactivation during Sterilization

A computational procedure was developed (Ghani *et al.*, 1999a) for describing the changes in the concentration of live bacteria and its transient spatial distributions during the sterilization processing of canned food. The governing equations of continuity, momentum, and energy were solved together with that for bacteria concentration. The Arrhenius equation was used to describe the kinetics of bacteria death and the influence of temperature on the reaction rate constant as described in Ghani *et al.* (1999a)

Figure 14.2 shows the results of the simulation for a metal can filled with CMC, steam heated from all sides (at 121°C). Figure 14.2(a) shows that during the early stage of heating, the bacteria are killed only at locations close to the wall of the can, and are not influenced by the flow pattern (Figure 14.1(c)). Figure 14.2(b) and (c) shows the results of the simulation after longer periods of 1,157s and 2,574s, respectively. The bacteria concentration profiles are different from those observed at the beginning of the heating. The liquid and thus the bacteria carried within it at the SHZ locations are exposed to less thermal treatment than the rest of the product. Figure 14.2(b) and (c) shows that the bacteria deactivation is influenced significantly by both the temperature and the flow pattern (Figure 14.1).

2.3 Simulation of Vitamin Destruction during Sterilization

The analysis used to study the inactivation of bacteria was extended to cover the destruction of different types of vitamins during thermal sterilization (Ghani *et al.*

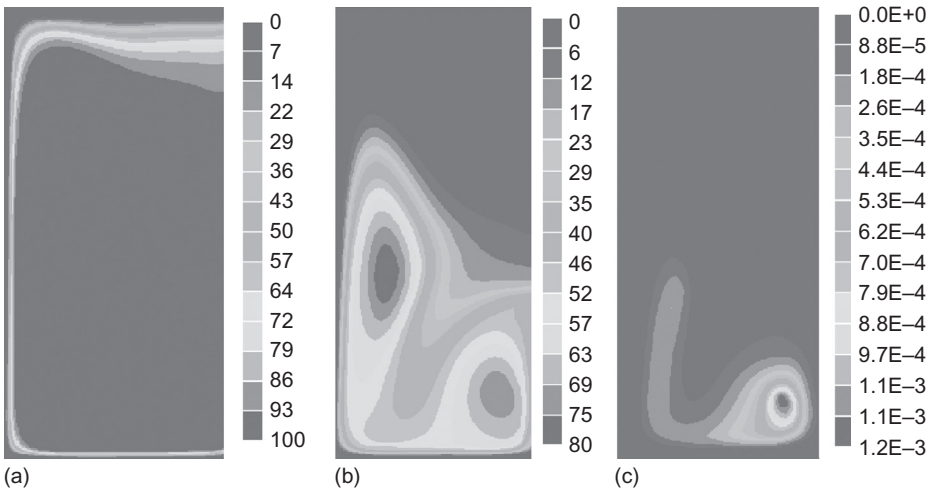

Figure 14.2 ***Deactivation of bacteria in a can filled with CMC and heated by condensing steam after 180s, 1,157s, and 2,574s, respectively. The right-hand side of each figure is centerline (Ghani et al., 1999b).***

2001). Profiles of concentrations of vitamin C (ascorbic acid), B1 (thiamin), and B2 (riboflavin) in a can filled with viscous liquid food (concentrated cherry juice) during thermal sterilization were presented and studied. The simulation highlights the dependency of the concentration of vitamins on both temperature distribution and flow pattern as sterilization proceeds (Figure 14.3).

2.4 Simulation of a Horizontal can during Sterilization

In this section, sterilization of a canned liquid food in a can lying horizontally and heated at 121°C from all sides is presented (Ghani *et al.*, 2000). Carrot–orange soup was used as the model liquid food. A non-uniform grid system was used in the simulation with higher mesh of 105,000 cells: 50 in the radial direction, 70 in the vertical direction, and 30 in the angular direction, graded with a finer grid near the wall in the radial and vertical directions. Because of the horizontal orientation of the cylindrical can used in this simulation, heat transfer is taken to be three-dimensional. The Navier–Stocks equations describing the system are presented in Ghani *et al.* (2002). Figure 14.4 shows the radial–angular temperature profile after 600s of heating. The can shown in this figure is in a horizontal position. The inclination shown is to more clearly show the 3-D image. This figure shows the actual shape of the slowest heating zone, which reduces gradually from the middle of the can toward the bottom surface.

2.5 Simulation of a 3-D Pouch during Sterilization

In this section, the simulation of a uniformly heated 3-D pouch containing carrot–orange soup is presented (Ghani *et al.*, 2001). As there is limited knowledge available on the

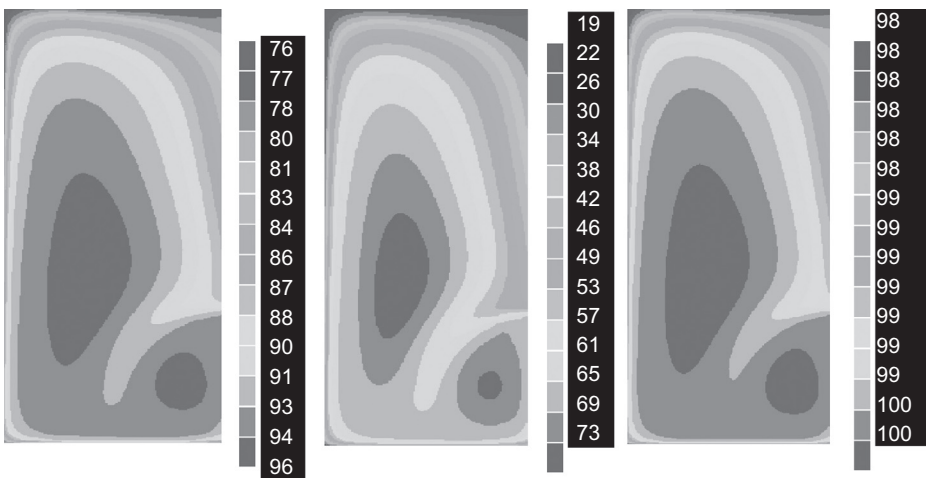

Figure 14.3 ***Vitamin destruction in a can filled with concentrated cherry juice and heated by condensing steam after 1,640s. The right-hand side of each figure is centerline (Ghani et al., 2001).***

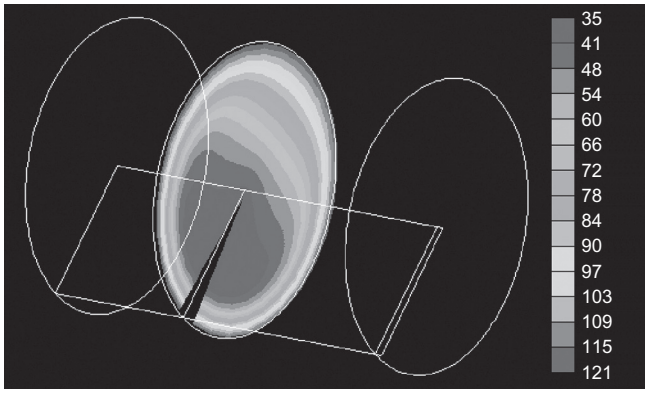

Figure 14.4 ***Radial–angular plane temperature profile of carrot–orange soup in a 3-D cylindrical can lying horizontally and heated by condensing steam after 600s (Ghani et al., 2002).***

sterilization of pouches, the investigation may be used to optimize the industrial sterilization process with respect to sterilization temperature and time.

The computations were performed for a 3-D pouch with a width of 120 mm, height of 35 mm, and length of 220 mm. The pouch volume was divided into 6,000 cells: 20 in the x-direction, 10 in the y-direction, and 30 in the z-direction (Figure 14.5). The partial differential equations governing natural convection of a fluid contained within a pouch are the Navier–Stocks equations in x, y, and z coordinates.

The result of simulation shows that the SHZ will not remain at the geometric center of the pouch as in conduction heating. As heating progresses, the SHZ is progressively pushed toward the bottom of the pouch as expected and eventually stays in a region about 30–40% of the pouch height. Figure 14.6 shows the temperature distribution at different y-planes in a pouch filled with carrot–orange soup at the end of heating (50 min).

3. CASE STUDY 2: NEW APPROACH TO THE ANALYSIS OF HEAT AND MASS TRANSFER IN DRYING AND FRYING

The common approach usually adopted to describe heat and mass transfer during drying is to solve numerically the heat conduction and mass diffusion equations within the drying material. An effective mass diffusivity is used to describe the diffusion of water and vapor through the solid. This is not true molecular diffusivity as it includes other diffusion mechanisms and was found to vary by more than one order of magnitude with the level of moisture content. Unfortunately, such diffusivity is difficult to measure experimentally and it is a function of moisture content, which limits the usefulness of such analysis.

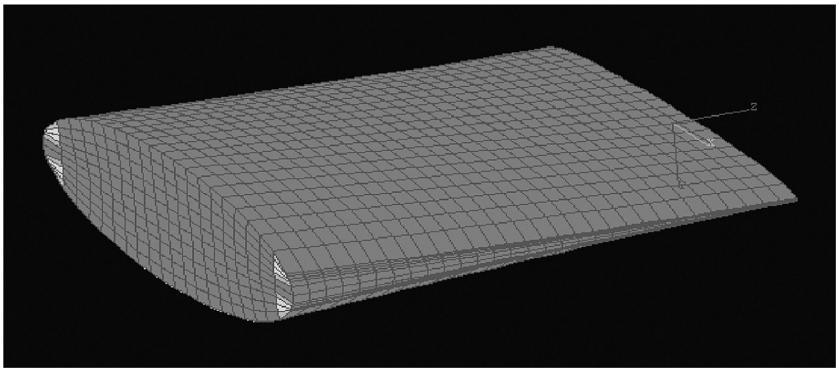

Figure 14.5 ***Pouch geometry and grid mesh (Ghani et al., 2000).***

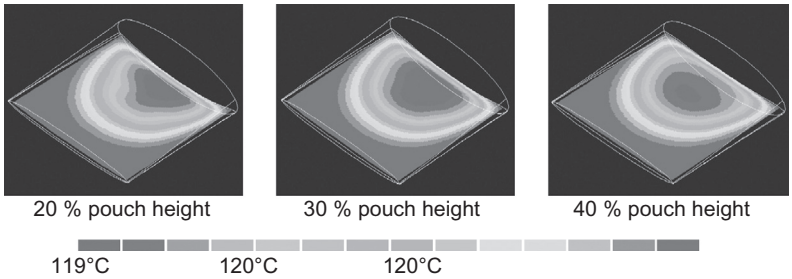

Figure 14.6 ***Temperature contours at different y-planes in a pouch filled with carrot—orange soup and heated by condensing steam after 50 min (Ghani et al., 2000).***

Farid has introduced a new approach to the analysis of heat and mass transfer during the different drying processes, including deep frying of foods in oil (Farid, 2001, 2002). The analysis was based on the formation of a moving interface, which acts as a heat sink where most of the heat is absorbed through water evaporation or sublimation. Although it may be difficult to describe air drying by this approach, because of the absence of a real sharp interface and the importance of mass diffusion, there are a number of other drying processes that may be described using a moving interface. Water evaporation, from moist solid such as foods, occurs at a receding interface during frying (Farid and Chen, 1998; Farkas *et al.*, 1996; Singh, 2000) air drying (Arzan and Morgan, 1967), and superheated steam drying (Li *et al.*, 1988; Schwartze *et al.*, 1988).

In freeze drying, water sublimation occurs with a moving interface at the water sublimation temperature that corresponds to the vacuum applied (Carn and King, 1977; Jafar and Farid, 2003; Sheng and Peck, 1975). In air drying, such as the spray drying of droplet containing solids, the moving interface may be defined by the air

wet-bulb temperature. In all these processes, heat must be conducted through the crust formed, which has a low thermal conductivity, before being absorbed at the interface. The water vapor generated at the interface will flow outward through the crust with little resistance in most of the applications.

Heat transfer in both the core (wet) and crust (dried) regions is described by the unsteady-state heat conduction Eq. 14.2. When moist materials are dried or fried, the core temperature will rise to the evaporation or sublimation temperature rapidly. Thus in most of these drying processes, the sensible heat of the materials can be ignored. For example, sensible heat accounts for $<2\%$ of the heat absorbed in frying and even less in freeze drying.

Most of the temperature distribution will occur within the crust because of its low thermal conductivity, which has been confirmed theoretically and experimentally in a number of drying applications reported in the literatures. The drying rate may be expressed in the case of flat geometry (Farid, 2001) as:

$$R = \frac{(T_\infty - T_{critical})}{\lambda\left(\frac{1}{h} + \frac{Y}{k_{cr}}\right)} \qquad [14.15]$$

If a modified Stefan Number is defined as $Ste = \frac{Cp(T_\infty - T_{critical})}{\varepsilon_o \lambda}$, a modified Fourier Number as $Fo = \frac{k_{cr} t}{\rho Cp}$, and a modified Biot Number as $Bi = \frac{hL}{k_{cr}}$, then Eq. 14.2 may be written in a dimensionless form:

$$R^* = \frac{1}{(\sqrt{1 + 2SteFoBi^2})} \qquad [14.16]$$

where the drying/frying rate (R^*) is defined as the ratio of the rate of drying at any time to the initial rate (usually known as the constant drying period, before crust is formed). This equation can be used to calculate the rate of drying at any time as the initial rate can be easily calculated from Eq. 14.14 by substituting $Y = 0$.

Some of the experimental measurements available in the literature on frying of thick and thin potato chips, freeze drying of slices of frozen beef, and air drying of potato chips were used to test the validity of the model.

Eq. 14.15 was used to calculate the dimensionless drying/frying rate (Figure 14.7) and it is evident that there is good agreement with the experimental measurements. The rate of heat transfer drops rapidly with time during the frying processes, as heat transfer is mostly controlled by heat conduction through the crust as a result of the high external heat transfer coefficient. Much slower drop in the rate is observed during air drying, because of the important role of the external heat transfer in such a process.

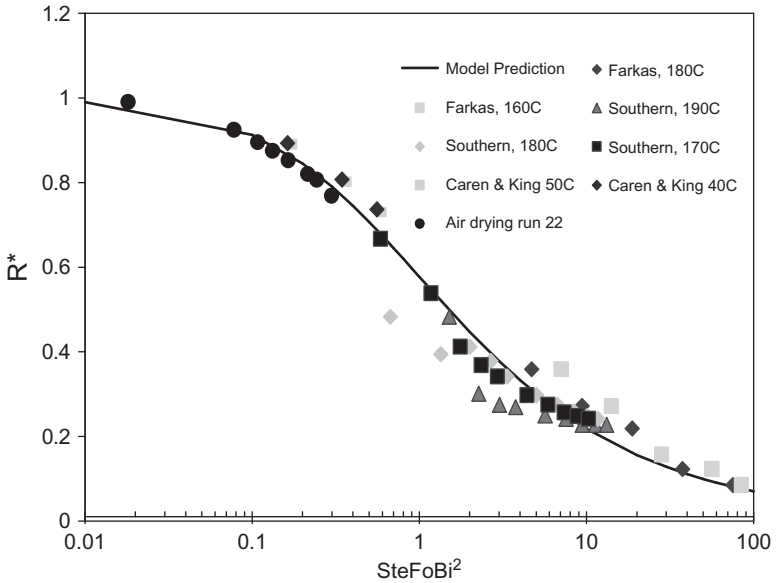

Figure 14.7 ***Model prediction of the dimensionless rate of frying, freeze drying, and air drying (Farid, 2001).***

The above analysis of drying and frying has been conducted based on planar geometry. For spherical and cylindrical geometry, we refer to the analysis presented by Smith and Farid (2004) who have reached the following dimensionless equation, which can be used to calculate the time needed for complete drying/frying:

$$Fo = \frac{R}{Ste} + \frac{P}{Bi.Ste} \qquad [14.17]$$

where Fo is defined in terms of the time needed for complete drying/frying.

The above equation is the same as that developed by Plank in the 1940s for freezing, including the values of the constants P and R, which are shown in Table 14.1 for the different geometries.

Figure 14.8 is a generalized plot of the dimensionless time (Fo) required for complete drying of all the measurements tested, which includes frying of potato crisps, cylinders and spheres, freeze drying of meat and potato, spray drying of droplets containing solids, and superheated steam drying of tortilla chips. The drying/frying time in these experiments varied from a few seconds as in the frying of thin potato crisps to many hours in freeze drying. Also, the Biot number varied from infinity for freeze drying of meat, 7 to 78 for frying of potato samples, and 0.3 for spray drying. Considering such large experimental variations, the agreement between the model and the experimental results may be considered to be good.

Table 14.1 Values of P and R for Various Geometries used in the Correlation

Geometry	R	P
Infinite slab	1/8	1/2
Infinite cylinder	1/16	1/4
Sphere	1/24	1/6

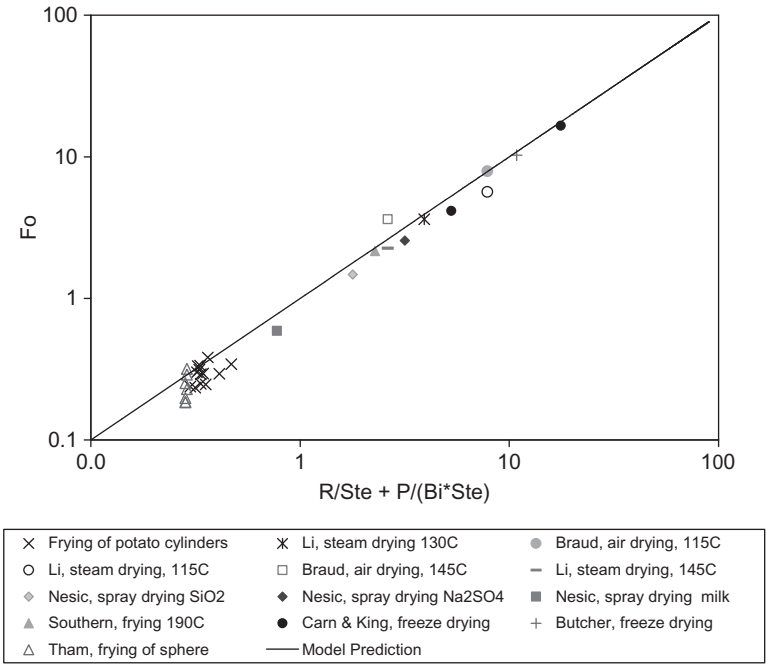

Figure 14.8 ***Model prediction of the time required for complete frying, freeze drying, superheating steam drying, air drying, and spray drying (Smith and Farid, 2004).***

4. CASE STUDY 3: MICROWAVE THAWING OF FROZEN MEAT

Thawing of frozen materials is important in food processing, while freezing is a convenient way of preserving food. Minimizing thawing times will reduce microbial growth, chemical deterioration, and excessive water loss caused by dripping or dehydration. Electromagnetic radiation in the frequency range from 300 MHz to 300 GHz is referred to as "microwaves". Microwave energy is used as a heat source in applications such as heating, drying, sterilization, and thawing of foods. The capability of a food product to heat when exposed to microwaves is dependent on its dielectric loss coefficient, which reflects the limit of the material to convert electromagnetic field into thermal energy. Frequencies commonly used for microwave heating are 915 and

2,450 MHz. Domestic ovens operate at 2,450 MHz, with a corresponding wavelength of radiation in the medium equal to 12.24 cm ($\lambda_o = c/f$). Microwaves may provide fast, efficient, and uniform heating but problems such as runaway heating are also common. Tempering or partial thawing of meat products with microwaves is already practiced in the meat industry.

The major problem associated with the development of industrial microwave processing is lack of understanding of the interactions between microwave radiation and food materials. There is a lack of predictive models relating physical, thermal, and electrical properties of food materials to the transient temperature field distribution, which determines microbial safety and product quality (Mudgett, 1986).

Microwaves can rapidly thaw small pieces of meat, but difficulties arise with large masses of frozen meat, which are used in industrial processes. Thawing does not occur uniformly, and some parts of the meat may cook while others remain frozen. Applying cyclic heating may minimize the runaway heating. The thawing rate of a frozen sample depends on the sample's material properties, dimensions, and on the magnitude and frequency of electromagnetic radiation.

Microwave heating has been theoretically studied by a large number of investigators based on the solution of Maxwell's equation, which assumes that microwave radiation is isotropic and normal to the surface of the material to be heated. Hill and Marchent (1996) have reviewed the numerical and analytical techniques used to study microwave heating. However, the theoretical analysis of microwave thawing has not received sufficient attention until recently. Chamchong and Datta (1999a,b) and Taher and Farid (2001) have recently studied microwave thawing of tylose samples using different power levels and showed the effects of power cycling on the non-uniformity of thawing.

4.1 Theoretical Analysis

The 1-D unsteady-state heat conduction Eq. 14.2 must be modified to incorporate heat generation due to microwaves:

$$\rho Cp_e \frac{\partial T}{\partial t} = \frac{\partial}{\partial y}\left(k\frac{\partial T}{\partial y}\right) + Q(y) \qquad [14.18]$$

As the process is accompanied by phase change (thawing), an effective heat capacity (Cp_e) was applied to account for the latent heat. $Q(y)$ is the microwave energy absorbed at the different locations (y) in the meat sample, which is commonly related to the microwave surface absorption Q_0, as follows (Taher and Farid, 2001):

$$Q_{th}(y) = Q_0 e^{-(y/D_{pl})} \qquad [14.19]$$

where D_{pl} is the microwave penetration depth in the thawed region, m.

The microwave energy absorbed at the location of the moving interface (Y) may be defined by the following equation, based on the above equation:

$$Q_{th}(Y) = Q_0 e^{-(Y/D_{pl})} \quad [14.20]$$

Based on the energy absorbed at the moving interface as defined above, the following expression may be used to calculate the absorbed energy in the frozen region:

$$Q_f(y) = Q_0 e^{-(Y/D_{pl})} e^{-(y\ -\ Y)/D_{ps}} \quad [14.21]$$

where D_{pl} is the microwave penetration depth in the frozen layer and Q_{th} and Q_f are the microwaves absorbed in the thawed and frozen regions, respectively. The analysis requires an interface location (Y), which is defined as the position corresponding to maximum effective heat capacity. Measurements of thawing of meat show that this maximum effective heat capacity or enthalpy occurs at about $-2°C$ to $-3°C$, as will be described later.

By integrating the microwave heat absorbed in the two regions as defined by Eq. 14.18 and 14.20 with the assumption of total absorption of microwave, the following equation for the surface heat absorption due to microwave absorption (Q_0) is obtained:

$$Q_0 = \frac{(P/A)}{(1 - e^{-(Y/D_{pl})})D_{pl}(1 - e^{-(E-Y)/D_{ps}})D_{ps}} \quad [14.22]$$

where P/A is the microwave power per unit surface area exposed to radiation. Microwave penetration depth (D_{pl} or D_{ps}) is defined as the distance at which the microwave field intensity decreases to 37% of its incident value, which may be calculated from the following equation (Basak and Ayappa, 1997):

$$D_p = \frac{c}{2\pi f}\left(0.5K'\left(\sqrt{1+\left(\frac{K''}{K'}\right)^2}-1\right)\right)^{-1/2} \quad [14.23]$$

The penetration depth in the frozen region is calculated from the known values of K' and K'' (Table 14.2). The value of D_{ps} for the frozen meat is found to equal 0.064 m. For the thawed phase, values of K' and K'' are calculated as functions of the average temperature of the thawed phase (T_{av}), using the following equations (Panggrle *et al.*, 1991):

$$K' = 50.6 - 0.183T_{av} \quad [14.24]$$

$$K'' = 20.25 - 0.665T_{av} + 0.0096T_{av}^2 - 5 \times 10^{-5}T_{av}^3 \quad [14.25]$$

Table 14.2 Average Thermal and Dielectric Properties of Lean Beef

	Unfrozen Phase	Frozen Phase
Thermal conductivity	Eq. 14.30	Eq. 14.30
Density	1,057 kg/m^3	961 kg/m^3
Specific heat capacity	3.51 kJ/kg°C	2.09 kJ/kg°C
K'	Eq. 14.23	6.0
2,450 MHz K″	Eq. 14.24	1.5
D_p	Eq. 14.22	0.064 m

Eq. 14.18 to 14.22 may be used to calculate the rate of heat generation due to microwave absorption as a function of position within the meat sample.

According to the effective heat capacity method (EHC), the value of Cp_e is assumed to change within the thawing region such that

$$\int_{T_{m1}}^{T_{m2}} (Cp_e - Cp_e)dT = w\lambda \qquad [14.26]$$

where λ is the latent heat of freezing of water, w is the mass fraction of water in the meat, and T_{m1} and T_{m2} are the initial and final thawing temperatures, respectively.

The experimentally measured values of Cp_e are fitted to different polynomials at the different temperature ranges, as shown below (Taher and Farid, 2001):

$$Cp_e = 0.00007T^5 + 0.0061T^4 + 0.192T^3 + 2.9T^2 + 21.35T + 66.72 \quad \text{for } -4 \geq T \geq -25 \qquad [14.27]$$

$$Cp_e = 5.8T^3 + 62.83T^2 + 236.6T + 329.4 \quad \text{for } -2 \geq T \geq -4 \qquad [14.28]$$

$$Cp_e = 153.46T + 368 \quad \text{for } -1.4 \geq T \geq -2 \qquad [14.29]$$

$$Cp_e = -374T - 370.6 \quad \text{for } -1 \geq T \geq -1.4 \qquad [14.30]$$

The thermal conductivity of the frozen and thawed meat sample is calculated from the following equation, derived from the available experimental measurements (Mellor, 1978):

$$k = -0.0007T^4 - 0.0036T^3 - 0.0605T^2 - 0.431T + 0.489 \quad \text{for } 20 \geq T \geq -25 \qquad [14.31]$$

Eq. 14.17 is solved numerically in the frozen, thawed, and phase change (mushy) regions, using the corresponding physical properties of each phase. Explicit finite difference method with controlled stability is used for the numerical solution.

In this analysis, the meat is assumed insulated both thermally and from microwaves at its bottom and sides to maintain 1-D heating. Accordingly, zero heat flux is assumed at the bottom surface, while convective heating or cooling is assumed at the top surface, which is exposed to microwave radiation. The evaporative surface cooling is also included using the Chilton−Colburn Analysis.

The convection heat transfer coefficient calculated from correlations, available in the literature, is used to calculate the heat loss from the surface of the sample according to Newton's law of cooling:

At the surface ($x = 0$)

$$-k\frac{dT}{dy} = h(T_s - T_\infty) \qquad [14.32]$$

at the bottom insulated surface ($y = E$)

$$\frac{dT}{dy} = 0 \qquad [14.33]$$

During the early stages of thawing, heat transfer from the ambient has little effect on the thawing process. However, when the surface temperature rises significantly above the ambient, heat loss because of convection and evaporation causes some cooling on the surface and hence slows down the thawing process.

4.2 Discussion of Results

Complete thawing of meat by microwaves may not be practical because of excessive heating of the surface that is exposed to microwave heating. The simulation was conducted using controlled temperature heating (Figure 14.9). Microwave heating was stopped when the surface temperature reached 10°C, and it was started again when the surface temperature dropped below 10°C. The use of controlled surface temperature microwave thawing may reduce thawing times by more than one-fifth of those required by conventional thawing. Figure 14.9 shows that complete thawing has occurred after 100 min with the surface temperature not exceeding 10°C, and this helped to maintain the product quality. The corresponding time in conventional thawing, even under ambient temperature, is >500 min (Figure 14.10).

NOMENCLATURE

A	Heat and mass transfer area, m^2
Bi	Modified Biot Number, $Bi = hL/k_{cr}$ for slab or hr_0/k_{cr} for sphere
Ca	Concentration, kg m^{-3}
Cp	Specific heat capacity of the material core, J/kg K
Cp_e	Effective heat capacity of meat, J/kg K
Cp_s	Specific heat capacity of frozen meat, J/kg K

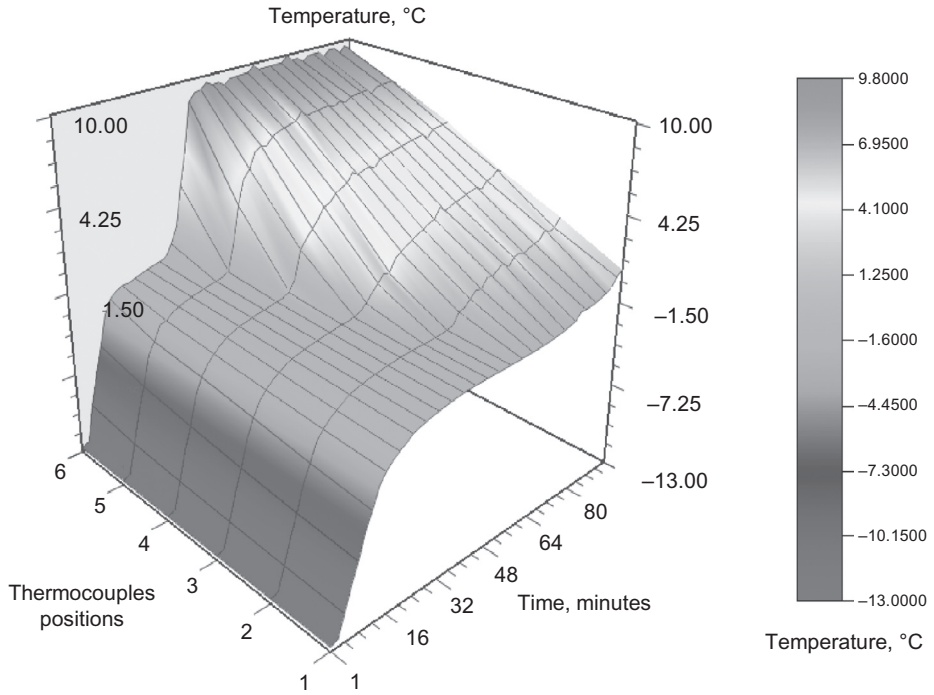

Figure 14.9 ***Model prediction for microwave thawing of 1.5 kg frozen meat sample with 28% power rating and surface temperature controlled (Taher and Farid, 2001).***

d	Ordinary derivative
D	Diffusivity, $m^2\ s^{-1}$
Dpl	Penetration depth of the thawed phase, m
Dps	Penetration depth of frozen phase, m
E	Meat sample thickness, m
F	Radiation shape factor, dimensionless
Fo	Modified Fourier Number, $Fo = k_{cr}t/(\rho Cp)$
h	Heat transfer coefficient, $W/m^2\ K$
hm	Mass transfer coefficient
K′	Relative dielectric constant (dimensionless)
K″	Relative dielectric loss (dimensionless)
K	Thermal conductivity, W/m K
k	Thermal conductivity, W/m K
k_{cr}	Thermal conductivity of crust, J/s mK
L	Characteristic dimension, m
m	Mass of material, kg
Nu	Nusselt number, hL/k
P	Microwave power, W
p	Pressure, Nm^{-2}
Pr	Prandtel number, Cpμ/k
q	Heat flow, W

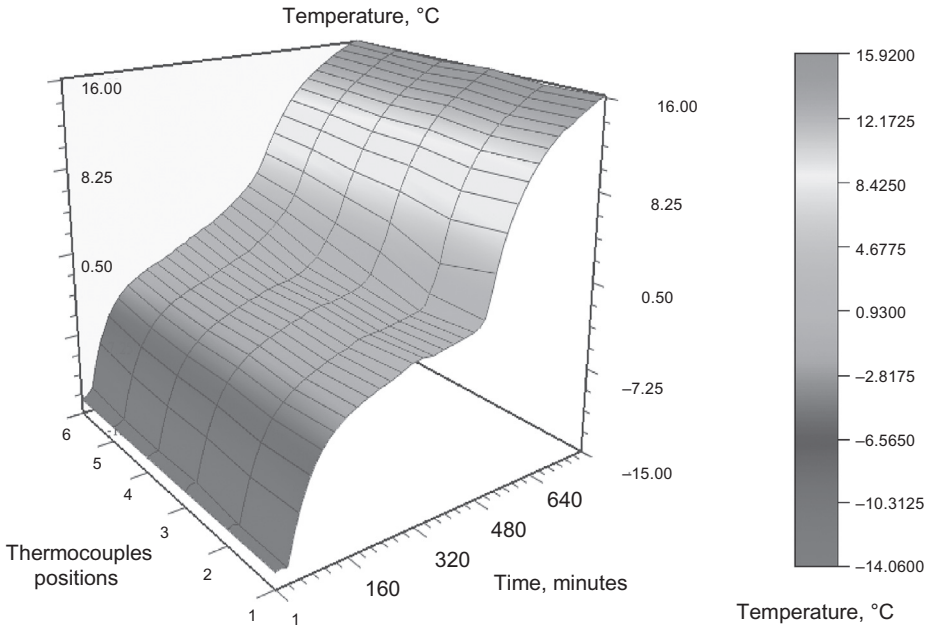

Figure 14.10 ***Experimental measurements for conventional thawing of 1.5 kg frozen minced beef sample with ambient temperature = 21°C (Basak and Ayappa, 1997).***

Q	Microwave heat absorption, W/m^3
Q_f	Microwave heat absorbed in the frozen region, W/m^3
Q_o	Microwave surface heat absorption, W/m^3
Q_{th}	Microwave heat absorbed in the thawed region, W/m^3
r	Radial position or coordinate
R	Drying/frying rate (defined by Eq. 14.14), kg water $m^{-2}\,s^{-1}$
R*	Dimensionless drying/frying rate (defined by equation 15)
Re	Reynold number, $\rho uL/\mu$
Ste	Modified Stefan Number, $S_{te} = Cp\,(T_\infty - T_{critical})\,/\,(\varepsilon_0\lambda)$
T	Time, s
T	Temperature, °C
T_∞	Ambient temperature, °C
T_{av}	Average temperature $T_{av} = (T_s + T_m)/2$, °C
T_i	Initial temperature, °C
T_{m1}	Initial melting temperature, °C
T_{m2}	Final melting temperature, °C
T_∞	Fluid bulk temperature, °C
T_s	Surface temperature, °C
$T_{critical}$	Solidification, sublimation, evaporation, or wet-bulb temperature, °C
v, u	Velocity, $m\,s^{-1}$
W	Water content, kg water/kg meat
y	Position from surface, m
Y	Interface position, m

GREEK SYMBOLS

α Thermal diffusivity, $m^2\ s^{-1}$
β Thermal expansion coefficient, K^{-1}
λ Latent heat of solidification, evaporation, or sublimation, $J\ kg^{-1}$
ρ Density, $kg\ m^{-3}$
∂ Partial derivative
ε_0 Initial free moisture content, kg water/kg total
ε_1 Emittance
σ Stefan Boltzmann constant, $W\ m^{-2}\ K^{-4}$
μ Dynamic viscosity, $kg\ m^{-1}\ s^{-1}$

REFERENCES

Arzan, A.A., Morgan, R.P., 1967. A two-region, moving boundary analysis of the drying process. Chem. Eng. Prog. Symp. 79 (63), 24–33.
Basak, T., Ayappa, K.G., 1997. Analysis of microwave thawing of slabs with effective heat capacity method. J. AIChE 43, 1662–1674.
Carn, R.M., King, C.J., 1977. Modification of conventional freeze dryers to accomplish limited freeze-drying. AIChemE Symposium Series No. 163, 73, pp. 103–112.
Chamchong, M., Datta, A.K., 1999a. Thawing of foods in a microwave oven: effect of power levels and power cycling. J. Microw. Power Electromag. Ener. 34, 9–21.
Chamchong, M., Datta, A.K., 1999b. Thawing of foods in a microwave oven: effect of load geometry and dielectric properties. J. Micro. Pwr. Electromag. Ener. 34, 22–32.
Farid, M.M., 2001. A unified approach to the heat and mass transfer in melting, solidification, frying and different drying processes. Chem. Eng. Sci. 56, 5419–5427.
Farid, M.M., 2002. The moving boundary problems from melting and freezing to drying and frying of food. Chem. Eng. Proc. 41, 1–10.
Farid, M.M., Chen, X.D., 1998. The analysis of heat and mass transfer during frying of food using a moving boundary solution procedure. Heat Mass Trans. 34, 69–77.
Farkas, B.E., Singh, R.P., Rumsey, T.R., 1996. Modeling heat and mass transfer in immersion frying. II, model solution and verification. J. Food Eng. 29, 227–248.
Ghani, A.G., Farid, M.M., Chen, X.D., Richards, P., 1999a. An investigation of deactivation of bacteria in canned liquid food during sterilization using computational fluid dynamics (CFD). J. Food Eng. 42, 207–214.
Ghani, A.G., Farid, M.M., Chen, X.D., Richards, P., 1999b. Numerical simulation of natural convection heating of canned food by computational fluid dynamics. J. Food Eng. 41, 55–64.
Ghani, A.G., Farid, M.M., Chen, X.D., 2000. Thermal sterilization of canned food in a 3-D pouch using computational fluid dynamics. J. Food Eng. 48, 147–156.
Ghani, A.G., Farid, M.M., Chen, X.D., Richards, P., 2001. A computational fluid dynamics study on the effect of sterilization on bacteria deactivation and vitamin destruction. Proc. Inst. Mech. Eng. 215 (E), 9–17.
Ghani, A.G., Farid, M.M., Chen, X.D., 2002. Numerical Simulation of transient temperature and velocity profiles in a horizontal can during sterilization using computational fluid dynamics. J. Food Eng. 51, 77–83.
Hill, J.M., Marchent, T.R., 1996. Modeling microwave heating. Appl. Math Model. 20.
Holman, J.P., 1992. Heat Transfer, seventh ed. McGraw-Hill, New York.
Jafar, F., Farid, M.M., 2003. Analysis of heat and mass transfer in freeze drying. Dry. Tech. Internat. J. 21, 249–263.

Li, Y.B., Yagoobi, J.S., Moreira, R.G., Yamasaengsung, E., 1988. Superheated steam impingement drying of tortilla chips. Drying 1998: Proceedings of the Eleventh International Drying Symposium, pp. 1221–1228.
Mellor, J.D., 1978. Thermophysical properties of foodstuffs: 2. Theoretical aspects. Bull. IIR 58, 569.
Mills, A.F., 1992. Heat Transfer. Richard Irwin, Inc, Boston.
Mousa, N., Farid, M.M., 2002. Microwave vacuum drying of banana slices. Drying Tech. 20, 2055–2066.
Mudgett, R.E., 1986. Microwave properties and heating characteristics in foods. Food Tech. 40, 84–93.
Ozkan, N., Ho, I., Farid, M.M., 2004. Combined ohmic and plate heating of hamburger patties: quality of cooked patties. J. Food Eng. 63, 141–145.
Panggrle, B.P., Ayappa, K.G., Davis, H.T., Gordon, J., 1991. Microwave thawing of cylinders. J. AlChE 37, 1789.
Schwartze, J.P., McKinnon, A.J., Hocker, H., 1988. Experimental investigation of the through-drying of fibrous mats with superheated steam. Drying 1998: Proceedings of the Eleventh International Drying Symposium, pp. 1637–1644.
Shafiur, R., 1995. Food Properties Handbook. CRC Press.
Sheng, T.R., Peck, R.E., 1975. A model of freeze drying of foods and some influence factors on the process. AlChE Symposium Series, 37, pp. 124–130.
Singh, R.P., 2000. Moving boundaries in food engineering. Food Tech. 54, 44–53.
Smith, M.C., Farid, M.M., 2004. A single correlation for the prediction of dehydration time in drying and frying of samples having different geometry and size. J. Food Eng. 63, 265–271.
Taher, B.J., Farid, M.M., 2001. Cyclic microwave thawing of frozen meat: experimental and theoretical investigation. Chem. Engin. Proc. 40, 379–389.
Treybal, R.E., 1980. Mass Transfer Operation, second ed. McGraw-Hill, New York.